Completing the Inventory of the Solar System
ASP Conference Series, Vol. 107, 1996
T. W. Rettig and J. M. Hahn, eds.

Planetary Accretion

William R. Ward
Jet Propulsion Laboratory, California Institute of Technology, Pasadena, CA 91109

Abstract. This paper reviews current ideas concerning the planetary formation process. An order of magnitude discussion is presented, concentrating on the principal concepts that comprise present models. The overall accretion process can be partitioned into three stages, each dominated by different mechanisms and/or styles of accumulation. Characteristic time scales are estimated for each stage and compared with the probable lifetime of the primordial nebula. Several ideas for shortening or eliminating the slow, problematic late-stage are discussed.

1. Introduction

This paper reviews what are currently believed to be the salient features of the planet building process. The discussion is an order of magnitude approach, concentrating on key issues and indicating where significant gaps in our understanding persist. The overall sequence of events can be conveniently split into three stages through the definition of two characteristic masses for a planetesimal disk. Each of these stages is dominated by different mechanisms and/or styles of accumulation. Table I provides an overview of these stages and processes in question.

The next section deals with early-stage growth, during which the solid material fractionates from the gas and settles into a thin planetesimal disk in the nebula's mid-plane. During this stage, accumulation mechanisms are largely non-gravitational in nature. Section III describes the mid-stage, which is, perhaps, the most thoroughly studied and best understood. It is dominated by binary accretion among planetesimals large enough that their individual gravitational fields are not negligible and by runaway growth, which is a consequence of gravitational focussing and keplerian shear. In section IV, the problematic late-stage is discussed, where close encounters between planetesimals and planetary embryos can no longer be assured by the keplerian motion of the disk alone. If further collisions require large eccentricities and inclinations to generate crossing orbits, the resulting low collision probabilities imply that this stage is the longest in duration and, thus, sets the overall time scale for planetary formation. Indeed, this apparently introduces a time scale dilemma for the formation of the giant planets. The giant planets are thought to develop by first forming a solid core through binary accretion. When this core is of sufficient size, i.e 10-20 earth masses, a rapid gas accretion stage initiates, eventually adding most of their mass. Because the implied accumulation time for their cores is well in

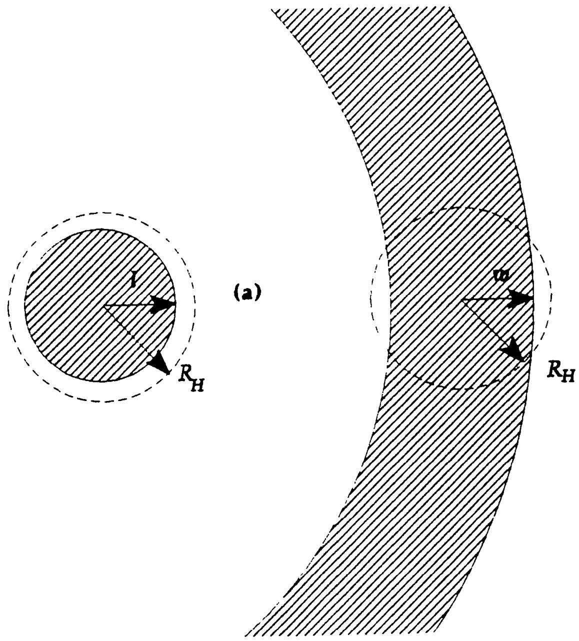

Figure 1. Characteristic masses for a planetesimal disk. a.) self-gravity dominates shear stress in the disk over an area of radius, l, containing a mass, $m_1 = \pi\sigma l^2$. b.) keplerian motion alone can continue to generate close encounters over a annulus of half-width, w, containing a mass, $m_2 = 4\pi r\sigma w$.

excess of the probable $\sim \mathcal{O}(10^7)$ year lifetime of the gas disk, their exist prior to disk dispersal is hard to reconcile. Some possible resolutions to this time scale problem will be discussed. The paper then concludes with a brief summary and suggestions for further work.

Before beginning our discussion, we shall provide simple derivations the characteristic masses that can be used to define the stage boundaries (Hourigan and Ward, 1974). Consider a particulate disk of surface density, σ, orbiting a primary, M_p, at a distance r with keplerian orbital angular velocity Ω. Choose a circular area of the disk of radius, l, (see Fig. 1a) encompassing a mass $m = \pi\sigma l^2$, which has an associated Hill's radius $R_H = r(m/3M_\odot)^{1/3}$. Define the first characteristic mass by requiring $l = R_H$, and solving for m self-consistently to obtain

$$m_1 = \pi\sigma r^2(\mu_d/3)^2, \qquad l = r(\mu_d/3) \tag{1}$$

where $\mu_d \equiv \pi G\sigma/r\Omega^2 = \pi\sigma r^2/M_p$ represents the so-called normalized disk mass. The length given by eqn (1) is a measure of the scale over which the disk's self-gravity dominates shear stresses in the disk. For specificity, values believed appropriate for the jovian zone in the primordial solar nebula will be employed throughout this discussion and are listed in Table II. Using a one solar mass primary, $M_p = M_\odot = 2 \times 10^{33}$ g, and $\mu_d = 3.5 \times 10^{-5}$, yields the characteristic length $l \simeq 10^9$ cm and mass, $m_1 \simeq 10^{19}$ g. This corresponds to a solid planetesimal with a radius of several kilometers.

The second characteristic mass is found by replacing the local area with an *annulus* of half-width, w, and mass $m = 2\pi r\sigma(2w)$ surrounding the primary (Fig. 1b). Setting $w = R_H$ then yields

$$m_2 = 8\pi\sigma r^2(\mu_d/3)^{1/2}, \qquad w = 2r(\mu_d/3)^{1/2} \tag{2}$$

This length is a measure of the radial scale over which keplerian shear can force close encounters among planetesimals. Using the values of Table II yields $w \simeq 5 \times 10^{11}$ cm and $m_2 \simeq 2 \times 10^{27}$ g. This mass corresponds to an planetary embryo with a radius of several thousand kilometers.

Table 1. Solid body accretion stages and some associated processes.

Early stage:	μm$\rightarrow$km	chemical condensation
		van de Waals bonding
		electrostatic/magnetic forces
	$\tau \sim \mathcal{O}(10^2\text{–}10^4)$ years	fluffy (fractal) aggregates
		compaction
		gas drag, settling to mid-plane
	$M \sim \mathcal{O}(10^{18}\text{–}10^{20})$ g	gravitational instability
		turbulence
Mid-stage:	km$\rightarrow$ $\mathcal{O}(10^3)$ km	gravitational scattering
		inelastic collisions
	$\tau_{acc} \sim \mathcal{O}(10^8\text{–}10^9)$ years	velocity damping by drag
	(orderly growth)	dynamic equilibrium
		fragmentation
	$\tau_{R'} \sim \mathcal{O}(10^6\text{–}10^7)$ years	binary accretion
	(runaway growth)	gravitational focusing
		dynamical friction
	$M \sim \mathcal{O}(10^{27}\text{–}10^{28})$ g	enhanced cross section
		accretion runaway
Late stage:	$\mathcal{O}(10^3)$ km$\rightarrow$planetary cores	high eccentricities?
		large impacts
	$\tau_{acc} > \mathcal{O}(10^9)$ years	radial mixing
	(orderly growth)	ejection from the
		solar system
	$\tau_{nebula} \sim \mathcal{O}(10^7)$ years	dissipation of nebula
		disk tidal torques
	$M \sim \mathcal{O}(10^{29}\text{–}10^{30})$ g	onset of gas accretion

2. Early Stage Growth

During the early stage ($m \leq m_1$) solid materials fractionate from the gas and settle to the mid-plane of the nebula, forming a planetesimal disk. The earli-

Table 2. Model parameters, Jovian zone

Heliocentric distance	r (5 AU)	7.5×10^{13} cm
Particle surface density	σ	4 g/cm^2
Gas surface density	σ_g	400 g/cm^2
Temperature	T	150 K
Keplerian frequency	Ω	1.8×10^{-8} s^{-1}
Keplerian velocity	$r\Omega$	1.3×10^{6} cm/s
Sound speed	c	9.3×10^{4} cm/sec
Gas scale height	$h = c/\Omega$	5.2×10^{12} cm
Normalized gas scale height	$h' = c/r\Omega$	0.07
Normalized planetesimal disk mass	$\mu_d = \pi\sigma r^2/M_\odot$	3.5×10^{-5}
Body density of planetesimal	ρ_p	~ 2 g/cm^3
Ratio of embryo radius to Hill radius	$d = R/R_H$	1.2×10^{-3}

est growth mechanisms do not rely on the gravitational attraction of individual particles, but on microphysical processes such as van der Waals bonding (e.g., Weidenschilling, 1980), electrostatic and/or magnetic forces, or possibly on interpenetration and compaction of highly porous and filamentary (fractal) structures (Donn, 1990). However, these processes work best in the sub-micron to millimeter size range and become less plausible for centimeter sized particles and larger.

The settling time scale and the size of the particles reaching the mid-plane depend in part on whether the nebula is turbulent. A large particle descending through a laminar nebula and sweeping up smaller particles along the way should reach the mid-plane with a radius $R \sim \mathcal{O}(\sigma/\rho_p) \sim$ a few centimeters in a time scale of a few orbital periods (Safronov, 1972; Goldreich and Ward, 1973). More detailed numerical models that track the particle size distribution give a somewhat larger maximum size (i.e. meters) and somewhat longer time scale (i.e., 10^2 orbit periods) for the formation of a particle layer (e.g., Weidenschilling, 1980; Nakagawa et al., 1983).

If the nebula is turbulent, particles must decouple from the gas before they can collect in the midplane. Turbulence can keep particles aloft, keeping their spatial density low and slowing their growth. If the turbulence is too strong, high relative velocities generated among the particles are more likely to fragment them than result in accretion. Their probable low impact strength, i.e., $\mathcal{O}(10^4$–$10^6)$ erg/cm^3, still renders it unlikely that particles much larger that a few centimeters will form (e.g., Weidenschilling, 1984; Mizuno, 1989; Blum and Munch, 1993).

Until recently, the gravitational instability mechanism enjoyed considerable popularity as an explanation for continued particle growth to several kilometers in size and, indeed, is closely related to our definition of m_1 (Safronov, 1972; Goldreich and Ward, 1973; Sekiya, 1983). Although the particles' individual gravity may be too weak to bind them upon collision, the collective gravitation attraction of a large number of particles may be sufficient to cause the planetesimal disk to break up into bound fragments. These fragments must be small enough that they are not disrupted by disk shear, but large enough to prevent evaporation of constituent particles. If the particles' dispersion velocity is less than $v_{crit} = \pi G\sigma/\Omega \simeq \mu_d r\Omega$, there is a range of fragment sizes, roughly centered on $\lambda = 2\pi^2 G\sigma/\Omega^2 = 2\pi\mu_d r$, that satisfy these conditions. In the jovian zone these values are $v_{crit} = 50$ cm/sec and $\lambda = 1.8\times10^{10}$ cm. By comparison, the escape velocity, $v_e \equiv \sqrt{2Gm/R}$, from a single particle is $\sim 7.5\times10^{-4}\rho_p^{1/2}(R/1\text{ cm})$ cm/sec. Thus, collective gravitational effects can promote accumulation at dispersion velocities much higher than the escape velocities of the constituent particle.

Weidenschilling (1980, 1988) has raised an important objection to the instability hypothesis. Because the nebula is partially pressure supported, it orbits at a slightly lower frequency than the planetesimal disk and a turbulent Ekman layer develops at the gas-particle interface (Goldreich and Ward, 1972). Weidenschilling warned that the boundary layer turbulence could sufficiently stir the planetesimal disk so as to keep the instability from developing. Following up this claim, Cuzzi et al. (1993) have developed a numerical two fluid model that simulates the interaction between gas and particles, including the effects of turbulence. They conclude that turbulence in the boundary layer maintains a dispersion velocity about an order of magnitude too high to allow the instability to set in. They suggest that accretion is, instead, driven by relative particle velocities that are induced by size dependent drag effects.

In a way, these results seem almost a setback. It is important to realize that a demonstration against gravitational instability does not itself *solve* the accretion problem. If the dispersion velocity exceeds the critical, v_{crit}, for instability, than it is clearly far above the escape velocities of individual centimeter to meter sized particles. Yet, no convincing explanation is offered for *why* such particles would accumulate rather then simply rebound, erode, or fragment as a result of their mutual collisions. (In fact, it was the absence of such an explanation that originally motivated the instability proposal to begin with (e.g., Goldreich and Ward, 1972)). The alternative "drift augmented accretion" scenario presented by Cuzzi et al. (1993), which is a variation of earlier work by Weidenschilling (1988), again suffers from this same deficiency.

Although several aspects of the early growth stage are still plagued with uncertainty, it is, nevertheless, generally believed that this stage was brief compared to subsequent stages of planetesimal growth, lasting of order 10^2–10^4 years. Consequently, the planetary accretion time scales are controlled by the later stages and in the next section, we shall pick up the story at the *mid-stage* where planetesimals with non-negligible gravitational fields, i.e., kilometers in radius, are assumed to have already formed so that further accretion *is* likely to proceed via inelastic binary collisions.

3. The Mid-stage

3.1. Binary Accretion

In its most basic formulation, the growth of a planetesimal is given by $\dot{R} = (mass\ flux) \times (cross\ section)$. The mass flux is $\simeq \rho v_{rel}$ where ρ is the spatial density of accretable material and v_{rel} represents a characteristic relative velocity among planetesimal in the disk. The scale height, h, of a planetesimal disk in collisional equilibrium scales with v, the particles' dispersion velocity, i.e., $h \sim v/\Omega$. If the relative velocities are also due to v, replacing $\rho \sim \sigma/2h$, yields a flux, $\sim \sigma\Omega$, that is insensitive to v. The velocity dependence of the growth rate enters through the cross section, πS^2, where S is the effective collision radius. The collision radius is generally larger than the physical radius, R, because of the target's ability to gravitationally focus the flux, i.e.,

$$S = R\sqrt{1 + (v_e/v_{rel})^2} \tag{3}$$

where v_e denotes the target's escape velocity. The ratio of the collision cross section to the geometrical cross section is sometimes referred to as the enhancement factor, F_g. For the simple binary model, $F_g = 1+(v_e/v_{rel})^2 = 1+8\pi G\rho_p R^2/3v_{rel}^2$, where ρ_p is the body density of the target. Eqn (3) can be easily modified to take into account finite sizes, R, R', of both projectile and target by replacing $R \rightarrow R + R'$ and $v_e^2 \rightarrow 2G(M + M')/(R + R')$.

What is the appropriate value of v? Safronov (e.g., 1969 and references therein) argued that the planetesimal disk would relax to an equilibrium state where the damping effects of inelastic collisions would be balanced by excitation of mutual gravitational scattering. The impact parameter for strong scattering is of order $\sim GM/v^2$ and requiring the strong scattering and collision cross sections to be comparable yields an equilibrium velocity of order $v \sim \sqrt{GM/\theta R}$, where θ is a constant called the Safronov number. The exact value of θ depends on the details of the model, such as the size distribution of the particles or whether there are additional damping mechanisms present such as gas drag, but is usually of order unity (e.g., Safronov, 1972; Kaula, 1979; Horedt, 1985). More detailed calculations of the velocity distribution have been developed using kinetic theory (e.g., Hornung et al., 1985; Stewart and Wetherill, 1988; Barge and Pellat, 1990; Ida, 1990) but parameterization by θ will be sufficient for our purposes. With this form for v; $v_{rel}^2 \sim 2v^2$, and the accretion rate becomes[1]

$$\dot{M} \simeq (\sigma\Omega)(\pi R^2)(1 + \theta). \tag{4}$$

In the ensuing discussion it will be useful to define a characteristic growth time; $\tau_j \equiv R/\dot{R}_j$ due to mechanism j. This can also be thought of as an estimate of the time interval a growing planetesimal spends at a given size. For binary accretion, eqn (4), the characteristic growth time reads,

$$\tau_{acc} \simeq \frac{\rho_p R}{\sigma\Omega}(1 + \theta)^{-1} \tag{5}$$

Figure 2 is a time scale diagram that shows $\tau_{acc} \simeq 4 \times 10^5(1 + \theta)^{-1}(R/\text{km})$ years, as a function of M (and R) for the values in Table II. [We have set $\theta \sim 1$, $\rho_p \sim 2$ g/cm^3 and included the constant $8\sqrt{3}$ in the definition of τ_{acc} (Lissauer and Stewart, 1993).] Also shown is the probable lifetime of the nebula. In the

[1]The often quoted rate which contains 2θ applies when one object is much larger than the other, so that the relative velocity is due mostly to the smaller object, i.e., $v_{rel} \sim v$. There are a variety of definitions for velocity in terms of orbital e's and I's; the reader is referred to Lissauer and Stewart (1993) for a good summary of current usages.

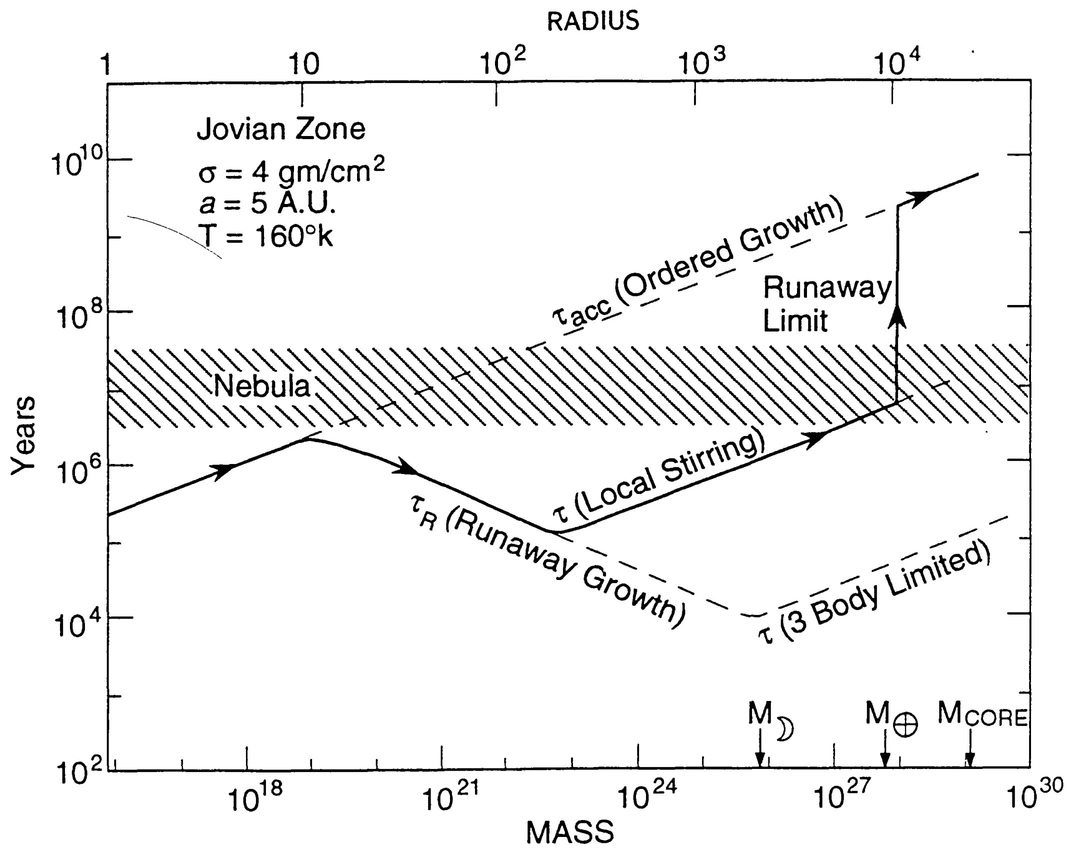

Figure 2. Time scale diagram for the jovian zone.

context of this diagram, our objective is to track the progress of an embryo up to the mass of a giant planet core *without* its evolutionary path, $\tau_j(M)$, rising above the nebula time boundary. We see immediately a possible dilemma: the time, τ_{acc}, to accrete a suitable giant planet core by binary accretion exceeds the probable lifetime of the gas disk by some two orders of magnitude.

3.2. Accretion Runaway

A partial resolution to this issue is furnished by the phenomenon of accretion *runaway*. Levin (1978) pointed out that an equilibrium disk could be unstable to the introduction of a larger planetesimal (embryo) with $M' \gg M, R' \gg R$ because of the strong feedback loop in the enhancement factor. If most of the mass resides in the small size range, the dispersion velocity will still be weighted toward the small particle escape velocities. In the case, the accretion rate for the embryo,

$$\dot{M}' \simeq (\sigma\Omega)(\pi R'^2)[1 + 2\theta(R'/R)^2] \tag{6}$$

is proportional to R'^4 when $(R'/R) \gg 1/\sqrt{2\theta}$. The characteristic growth time takes the form

$$\tau_{R'} \sim \frac{\rho_p R'}{\sigma\Omega(2\theta)}(\frac{R}{R'})^2 \simeq \tau_{acc}(\frac{R}{R'}). \tag{7}$$

Note that $\tau_{R'} \propto 1/R'$ and the embryo spends less and less time at a given size as it grows. A representative runaway track is shown in Figure 2, assuming that the developing embryo separates from the rest of the distribution when ordered growth has produced ~ 10 kilometer sized planetesimals. Provided runaway is initiated prior to nebula dispersal, this process appears capable of producing planetary sized embryos within the lifetime of the gas disk. The most time consuming part is in the initial phase of the runaway.

However, a key assumption has been made in eqn (7): that the relevant dispersion velocity used in the enhancement factor is controlled by the small sized particles in the swarm, $v \propto R$. If, instead, the velocity scales with the larger objects, $v \propto v_e' \propto R'$, the characteristic growth, $\tau_{R'} \propto R'$, and runaway does not develop. (The ratio R'/R would probably still increase, but this would be mostly due to a grinding down of small particles that are colliding at velocities much greater than their escape velocities.) Growth that more or less maintains the size distribution without the occurrence of runaway for some of its members is referred to as *ordered* growth. The early models of Safronov seem to largely fit into this category.

Whether ordered or runaway growth occurs depends on the behavior of the planetesimal velocities. However, the velocities depend on the evolving particle size distribution, which , in turn, depends on the accretion rates. One of the earliest attempts to quantitatively model this highly coupled problem was that of Greenberg et al. (1978, 1987). These authors devised a numerical code in which the particle size range was partitioned into a large number of discrete bins. The interactions of each bin population with all other bins was calculated using particle-in-a-box statistics. Both excitation and damping effects were included and a size dependent dispersion velocity determined for the occupants of each bin. If collisions predicted net growth, particles were promoted to larger bins. If fragmentation occurred, a distribution of smaller particles was added to lower mass bins in accordance fracture experiments. New bins were created at the upper and lower mass ends as needed. The particle swarm was followed until the assumptions underlying the particle-in-a-box statistics broke down.

The schematic diagrams in figure 3a,b taken from Greenberg (1989) illustrate the two evolutionary behaviors in question: ordered vs runaway growth. Assuming a starting power law distribution of the form $dN/dM \propto M^{-q}$, ordered growth would tend to preserve this functional form behind an advancing maximum size (Figure 3a). If the index, q, is less than 2, there is more mass in the larger size bins, which control the dispersion velocity. Conditions do not favor runaway and growth time scales are better approximated by τ_{acc} [eqn (5)]. Alternatively, Figure 3b shows a different evolution in which runaway develops. A small number of large objects (embryos) initiate accelerated growth and produce a steep, $q \gg 2$, power law wing at the upper mass limit of the original distribution. Most of the mass of the swarm still resides among the largest of the starting particles, which continue to control the dispersion velocity. Since this velocity is less than the escape velocity of the embryos, runaway growth continues. Which of these evolutionary tracks will actually be followed?

Figure 4 shows a typical output from the Greenberg et al. (1978) model. In this particular run, the starting distribution was actually a delta function at 1 kilometer. Within a very short time period, a few potential runaway objects develop from combinatorial statistics. These object quickly grow to $\sim 10^3$ kilometers while the bulk of the material is still near its original size. A small size

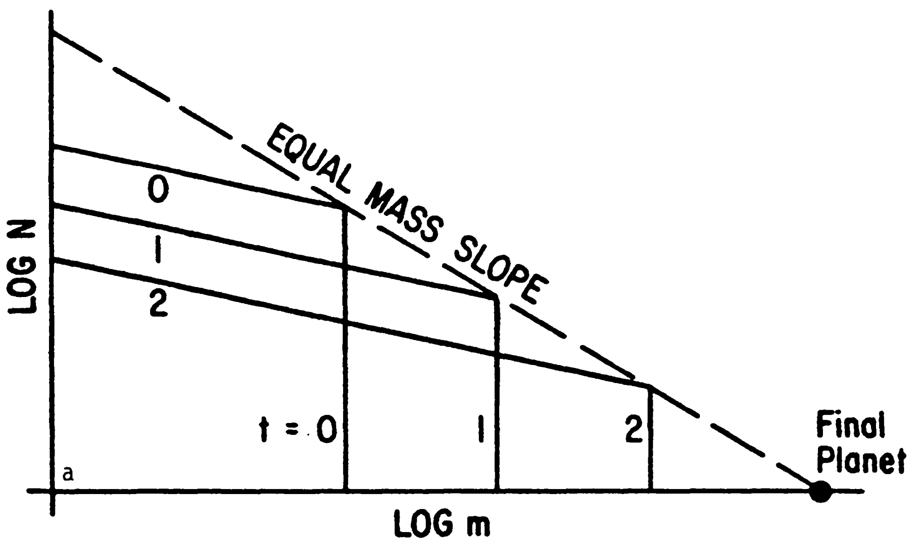

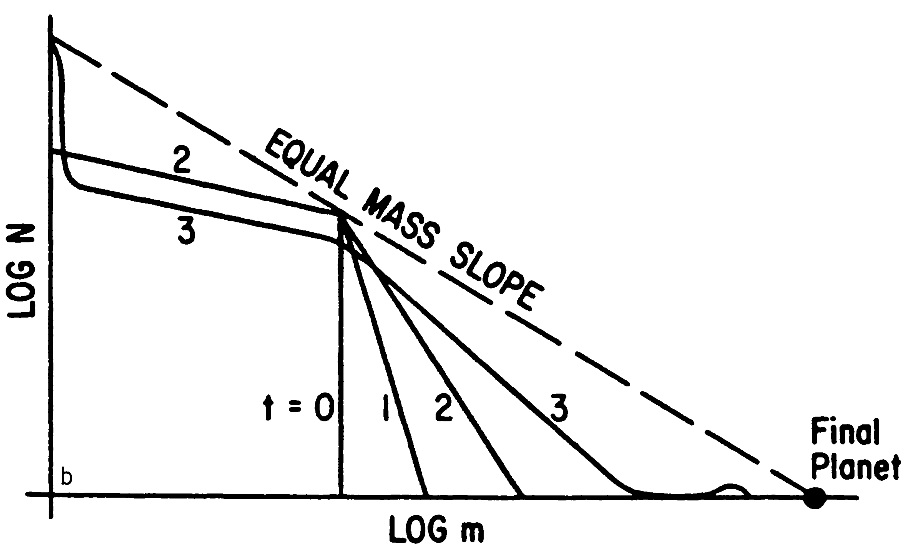

Figure 3. Schematic representation of a.) ordered growth and b.) runaway growth.

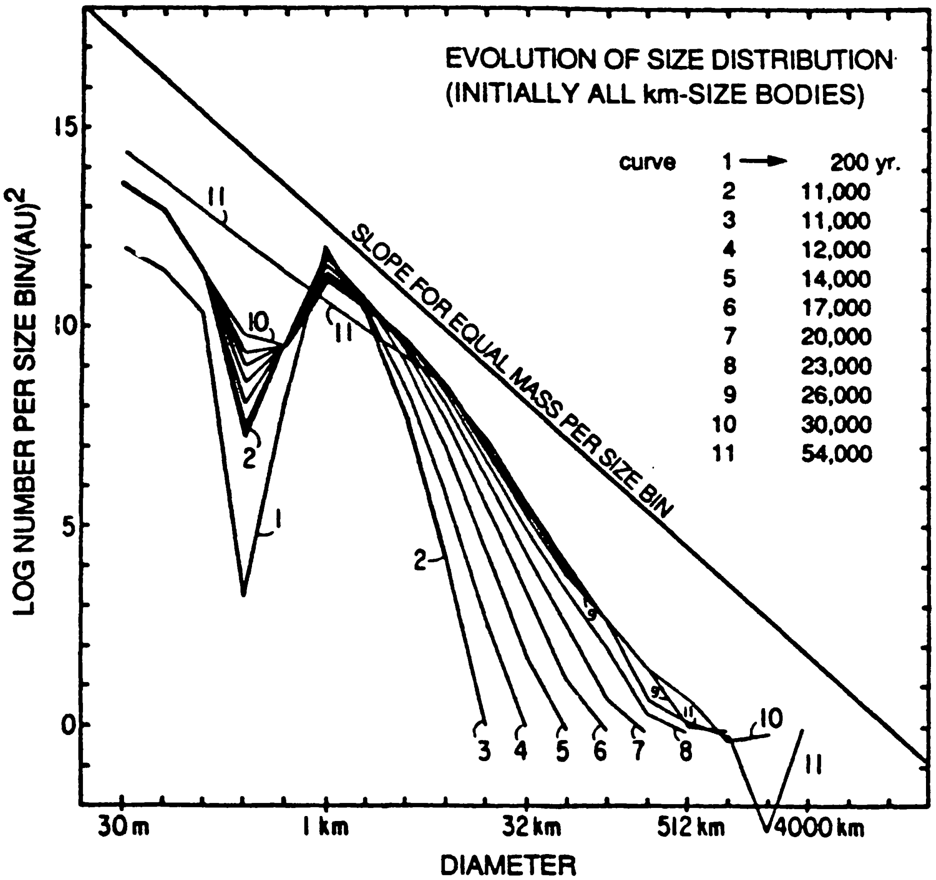

Figure 4. Evolution of planetesimal size distribution for numerical model of Greenberg et al., (1978).

tail due to fragmentation also develops, but contains only a minor amount of the system's mass. These results seemed to be convincing confirmation that accretion runaway was a likely outcome for a evolving planetesimal disk and that $\tau_{R'}$ [eqn (7)] is the more relevant time scale for growth of the largest objects during the mid-stage.

This problem has since been studied by several other researchers using both Monte Carlo techniques and N-body integrations. In particular, Wetherill and Stewart (1989, 1993) have developed a Monte Carlo code that includes a number of additional features pertinent to the accretion process including, dynamical friction, particle fragmentation, gas drag effects, seed bodies, independent tracking of planetesimal orbital eccentricities and inclinations, etc. Figure 5 shows two example cases, (a) one that displays ordered-type growth, and (b) one that develops runaway. Wetherill especially stresses the role of dynamical friction in promoting runaway for particles at the large end of the distribution. This was the key difference between these examples. Dynamical friction tries to establish energy equipartition among the particles so that larger mass objects acquire smaller dispersion velocities. This, in turn, increases their enhancement factor somewhat and contributes to runaway. Wetherill maintains that the original calculations of Greenberg and co-workers did not include this effect and are thus suspect. He suggests, instead, that the apparent runaway behavior found in these earlier models may have been an artifact of coding deficiencies, i.e., that

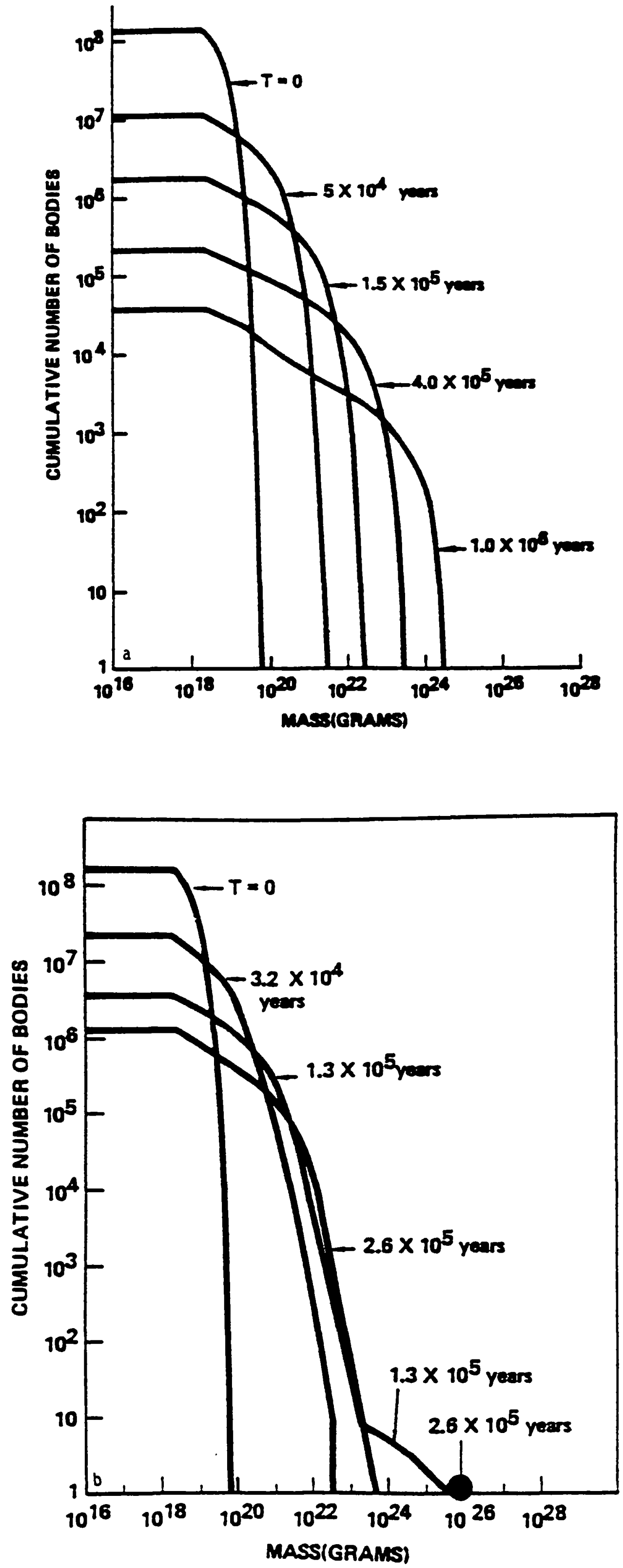

Figure 5. Evolution of planetesimal size distribution from Wetherill and Stewart (1989) for a.) ordered growth and b.) runaway growth.

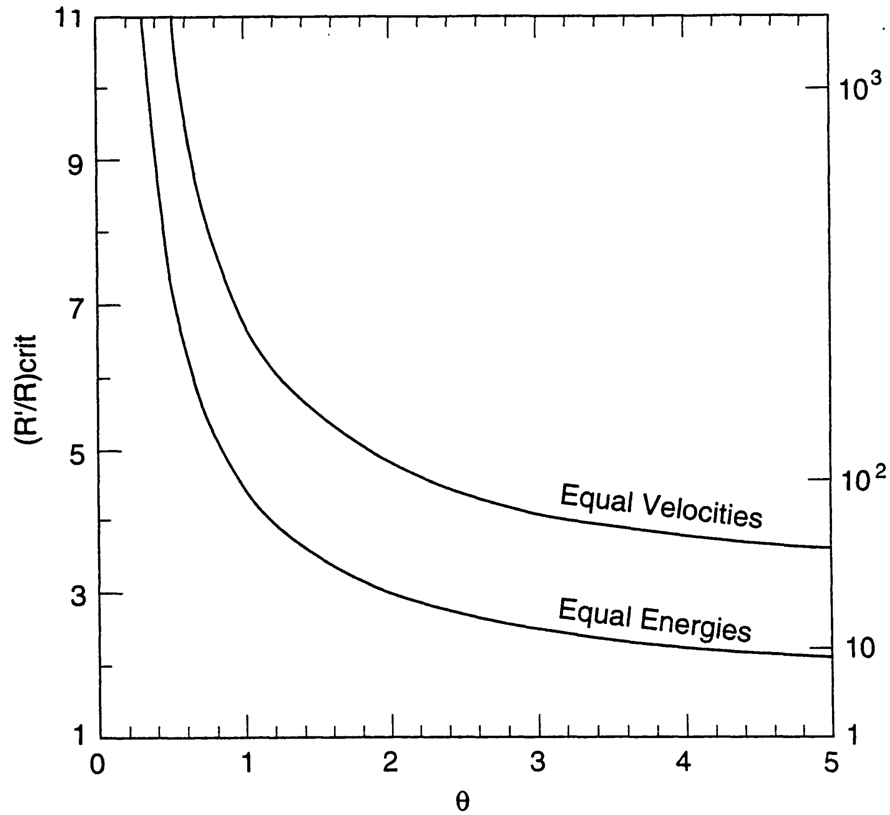

Figure 6. Critical size difference to initiate runaway as a function of Safronov number for equal velocities and for equal energies of embryo and field particles.

Greenberg et al. were right, but for the wrong reason. Similar concerns have been expressed by Spaute et al., (1991) and Ohtsuki et al. (1990) who have also developed numerical models that exhibit runaway. In response, Kolvoord and Greenberg (1992) have reexamined the original model and maintain that their algorithms did contain an adequate version of dynamical friction and that the accretion runaway found was a bona fide result.

Some idea of the relative importance of dynamical friction to the runaway issue can be found from Figure (6), which shows the critical size ratio R'/R, for which $d(R'/R)/dt$ becomes positive as a function of the field particles' Safronov number (see appendix). Cases with and without energy equipartition are shown. Equipartition does lower the critical ratio, but the effect is not dramatic. Although dynamical friction contributes to the likelihood of runaway, it does not seem quite as pivotal an issue as is sometimes claimed. Other factors, such as a stochastic growth of somewhat larger "seed" bodies, seems just as potentially important.

Regardless of who was the first to legitimately demonstrate the behavior, most workers now agree that runaway accretion is probably hard to prevent. This behavior is also found in the Monte Carlo type models of Ohtsuki and Ida (1990), Spaute et al. (1991), and Weidenschilling et al., (1993) and in the recent N-body models of Aarseth et al. (1993).

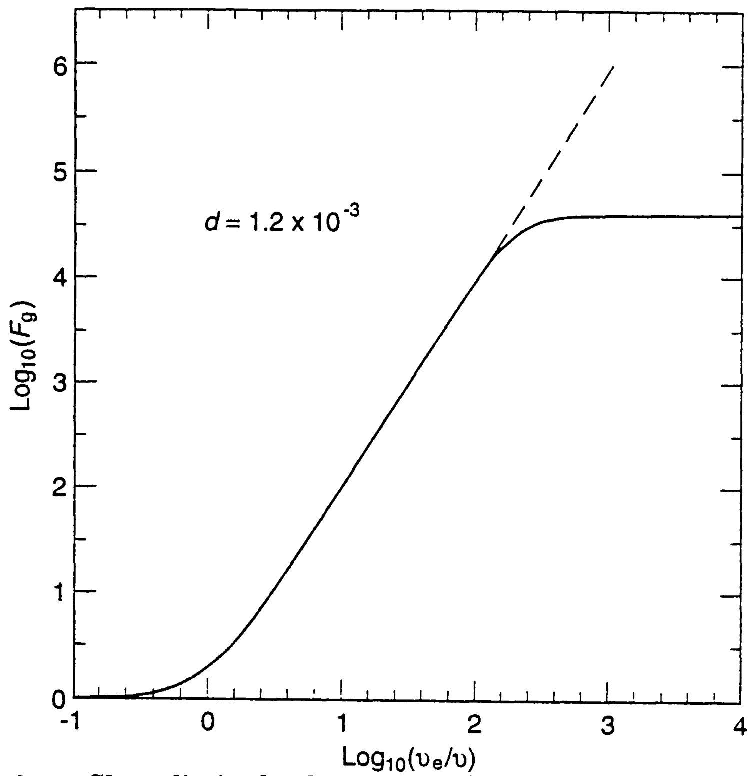

Figure 7. Shear limited enhancement factor obtained by substituting $v^2 \to v^2 + (3S\Omega/2)^2$ in the two-body formula for the effective collision radius.

3.3. Three Body Effects

However, the runaway growth rate cannot accelerate indefinitely. For example, the effective collision radius, S, could become so large that the relative velocity between projectile and target would become dominated by keplerian shear. A crude estimate of the shear limit can be made by replacing v_{rel}^2, in eqn (3) with $v^2 + (3S\Omega/2)^2$ and solving self-consistently (e.g., Weidenschilling, 1974; see also Ward, 1993);

$$(\frac{v_e}{v})^2 = \frac{F_g - 1}{1 - F_g(F_g - 1)(3R\Omega/2v_e)^2} \tag{8}$$

Figure (7) shows the resulting behavior of $F_g = (S/R)^2$ obtained by this simple procedure. For enhancement factors less than the maximum we recover the usual relationship, $F_g \sim 1 + (v_e/v)^2$. However, as $v_e/v \to \infty$, the effective radius approaches the limiting value, $S_\infty \sim \sqrt{2Rv_e/3\Omega}$. This implies an upper limit to the enhancement factor of $(2v_e/3R\Omega)^2 = F_g(F_g - 1) \simeq F_g^2$ so that

$$F_g \sim \frac{2}{3}(\frac{8\pi G\rho_p}{3\Omega^2})^{1/2} = \sqrt{\frac{8}{3d^3}} \simeq 4 \times 10^4 \tag{9}$$

where $d \equiv R/R_H \simeq 1.2 \times 10^{-3}$ is the ratio of the embryo's radius to its Hill sphere radius at 5 AU. Note that $S_\infty/R_H = d\sqrt{F_g} = (8d/3)^{1/4} = 0.24$, so that S_∞ is a fair fraction of the Hill radius.

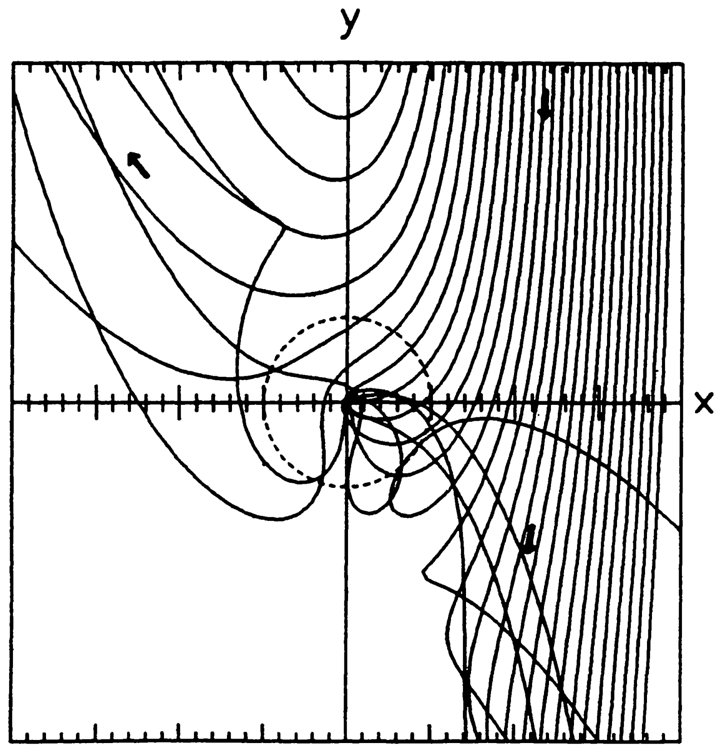

Figure 8. Encounter trajectories for particles approaching from circular orbits found by numerical integration of Hill's equations (Nishida, 1983).

Here a further word of caution is in order. The above estimate still treats the encounter as a two-body problem in which the target is in an inertial frame, emersed in a particle stream with a shear velocity field. The actual encounter is a three-body problem in which the solar tidal field plays an important role. This can be studied in detail through numerical integrations of Hill's equations, which contain centrifugal and Coriolis terms and describe the motion in a non-inertial frame rotating with the mean motion of the target. Figure (8) shows encounter trajectories as found by Nishida (1983) for particles approaching on circular orbits for a range of impact parameters. Many other researchers have reproduced versions of these results (e.g., Henon and Petit, 1985; Greenberg et al., 1988; Burns, 1989; Greenzweig and Lissauer, 1990; Ida et al., 1990). Note, that whereas the simple shear field calculations predict that objects with impact parameters less than S_∞ will collide with the target; in the three body calculation, such objects execute hairpin curves that are the end-points of horseshoe trajectories and never hit the target. Instead, impacting particles come from discrete bands located at $\sim \pm(2.0$ to $2.4)$ Hill sphere radii. Figure (9) displays the detail of these collision bands by plotting the distance of closest approach as a function of impact parameter as calculated by Henon and Petit (1985).

In order to quantitatively determine F_g, individual orbits must be numerically integrated to ascertain whether they strike the target and a careful inventory made. The ratio of actual impacts to that predicted for a geometrical cross section gives the true enhancement factor. Such a laborious procedure has been performed by Greenzweig and Lissauer (1990), the results of which are shown in Figure (10). The curve is qualitatively similar in behavior to Fig. (7) except

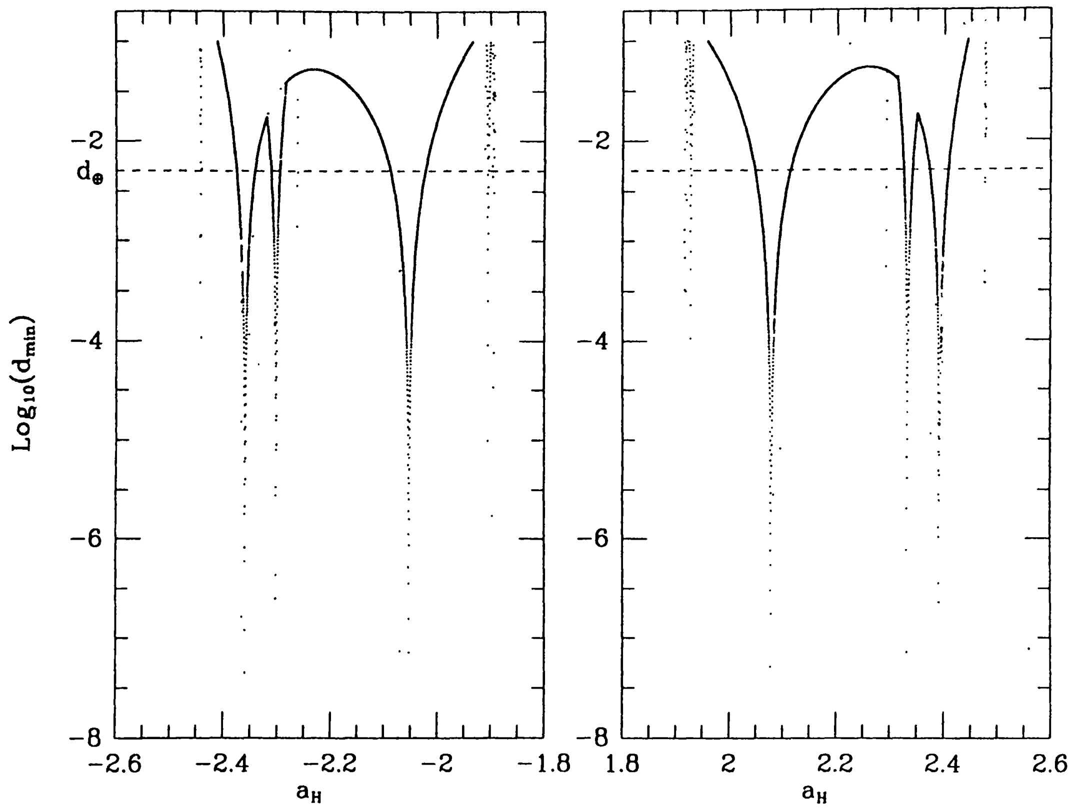

Figure 9. Closest approach distance in Hill radii of projectiles encountering target from circular orbits as a function of impact parameter. Approach distances closer than planet's surface, d, will impact planet.

that the limiting value of F_g is about a factor of three larger. Hence, although the three-body nature of the problem renders the detailed physics quite different, the final F_g value of is similar to that obtained from the simple shear flow estimate first made some twenty years ago! (Another interesting example of being right for the wrong reason.) An improved heuristic argument that agrees well with the numerical results has recently been provided by Greenberg et al. (1993).

Once F_g reaches its maximum value, the characteristic growth time reverts to a form linear in R',

$$\tau_{R'} \simeq \frac{\rho_p R'}{\sigma \Omega} \frac{1}{F_g} \simeq \frac{\tau_{acc}}{F_g} \tag{10}$$

as shown in Fig (2) for $F_g \sim 10^5$. Nevertheless, the time scale to form a suitable giant planet core still seems comfortably within the time constraint imposed by the nebula.

3.4. Stirring

Unfortunately, this is still probably overly optimistic. Lissauer (1987) speculated that even if most of the mass were contained in small particles, a large embryo

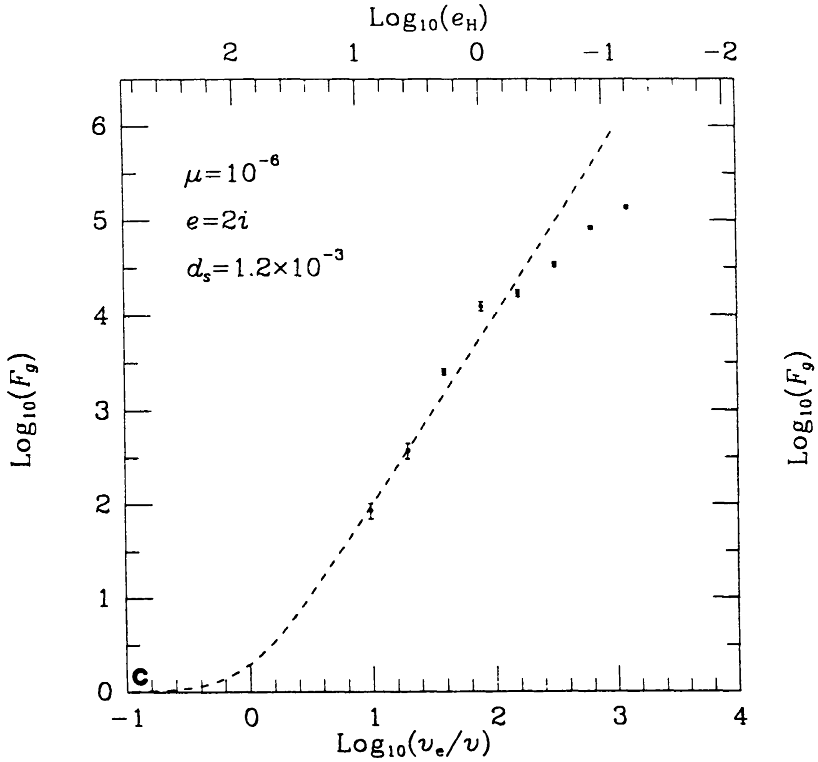

Figure 10. Enhancement factor as a function of dispersion velocity found by Greenzweig and Lissauer (1990) by numerical integration of Hill's equations.

will tend to stir the planetesimals swarm in its immediate vicinity. Planetesimal that make a close approach without an actual impact will re-encounter the embryo after an synodic period with a dispersion velocity on the order of the escape velocity from the Hill's sphere, $v \sim \mathcal{O}(R_H\Omega)$, (Greenzweig and Lissauer, 1990). Although for a single particle, conservation of the Jacobi constant, J, would guarantee the same relative velocity at each encounter; particle-particle interactions can change J during each synodic period. Recent numerical experiments conducted by Ida and Makino (1993) have largely confirmed this effect as shown in Fig (11). These authors have conducted N-body experiments in which a large embryo is surrounded by smaller planetesimals. They find that the larger object stirs up the dispersion velocities within an narrow annulus centered on the embryo with a half-width of a few R_H. This lowers the limiting enhancement factor to

$$F_g \sim (\frac{v_e}{\epsilon R_H \Omega})^2 \simeq \frac{2}{\epsilon^2}(\frac{12\pi G\rho_p}{\Omega^2})^{1/3} = \frac{6}{\epsilon^2 d} \tag{11}$$

where the value of ϵ depends on the details of the damping process, i.e., collisions, gas drag, etc. Using the values in Table 1, and $\epsilon \sim 2$ yields $F_g \sim 10^3$, i.e., about two orders of magnitude less than the three-body limit. The corresponding characteristic growth time of eqn (10) is also increased by $\sim 10^2$, and is shown in fig (2). The time scale to produce a planetary core is now only marginally within the time constraint imposed by the nebula. And even this time scale may not be applicable to full core size. Runaway growth may be inhibited by local mass exhaustion prior to achieving the requisite size.

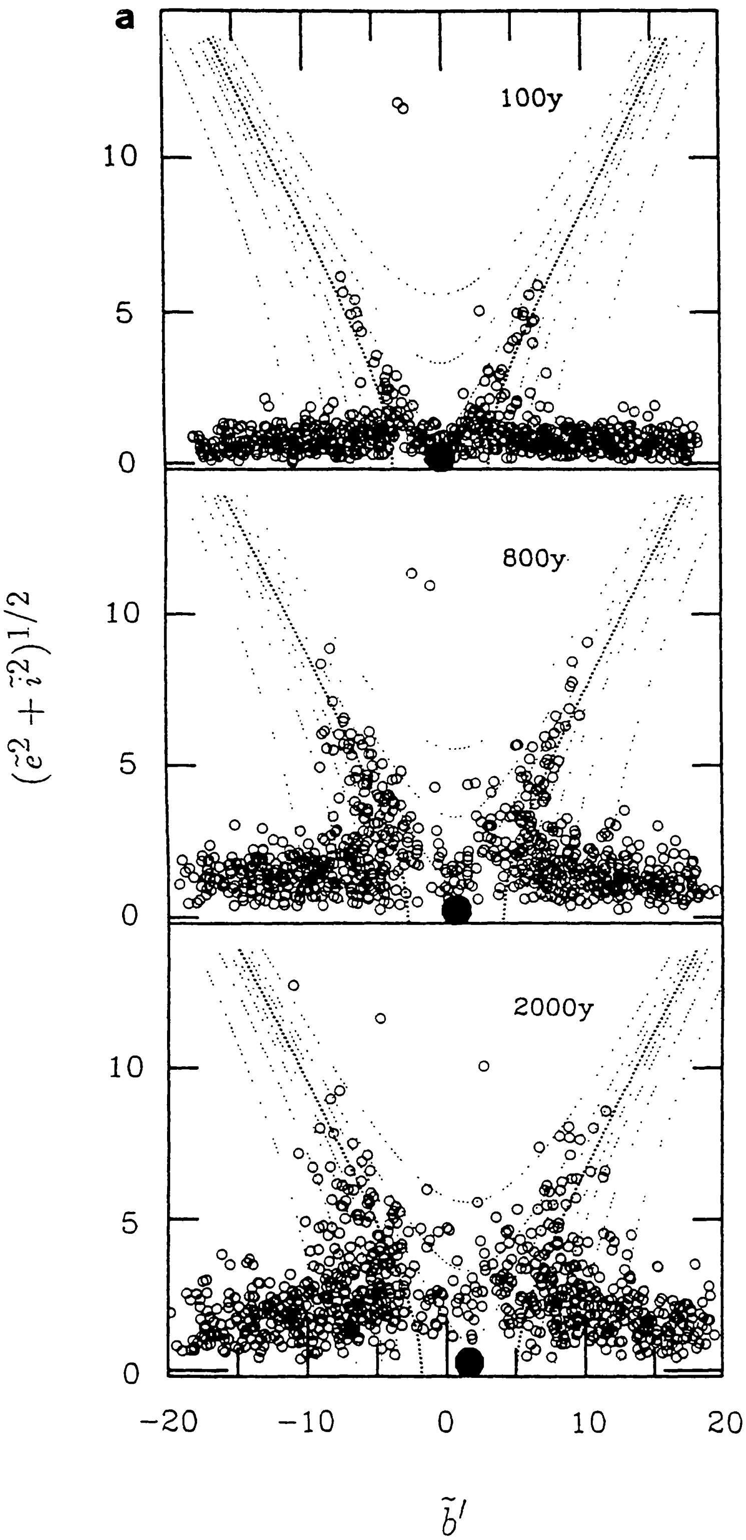

Figure 11. Stirring of smaller planetesimal by an embryo in N-body calculations of Ida and Makino (1993). Orbital elements are normalized to Hill radius, R_H. Stirring is confined to local region with a half-width of several R_H.

3.5. Runaway Limit

Dynamical friction causes embryo orbits to become very circular during their growth (e.g. Greenberg, et al., 1978; Stewart and Wetherill, 1988; Wetherill and Stewart, 1989). There is a minimum value of the Jacobi constant for a particle to pass through the Lagrange gates of the embryo's Hill's sphere (e.g., Hayashi, et al., 1977). For a planetesimal in an initially circular orbit, this corresponds to a differential semi-major axis of $\Delta a = 2\sqrt{3}R_H$. This has been interpreted as an effective accretion range (e.g., Lissauer, 1987; Artymowicz, 1987; Wetherill and Stewart, 1989; Wetherill, 1990; Lissauer and Stewart, 1993). On the other hand, the half-width of the cannibalized zone should scale linearly with the embryo's mass, $w \sim M/(4\pi\sigma r)$. These lengths are equal for

$$M_R = \sqrt[4]{3}(\frac{8\pi\sigma r^2}{M_\odot})^{3/2}M_\odot. \tag{12}$$

Note that this mass is within a constant of the secondary characteristic mass, m_2, defined in the introduction. Further growth must rely on diffusion of particles into the gap developing around the embryo (e.g., Hayashi et al., 1977, Artymowicz, 1987) or on some other mechanism, such as gas drag (e.g., Weidenschilling, 1977; Nakagawa et al., 1983) to supply new material, in which case the runaway time scale is no longer applicable. The jovian zone values yield, $M_R \sim 2M_\oplus$, which is about an order of magnitude too small for a giant planet core.

4. Late Stage Accretion

Mid-stage processes can account for rapid growth from $\sim 10^{18}$ to $\sim 10^{28}$ g, but appear to fall short of the desired core size by about an order of magnitude. Runaway growth has formally taken the evolution into the *late-stage* ($m_2 \leq m_R \leq m$), but in the remainder of this stage, some process(es) other than keplerian shear must ultimately be responsible for continuing to bring material into contact.

If crossing orbits are achieved by pumping up eccentricities and inclinations as in the Monte Carlo models of Wetherill (1980), further accretion should follow the stochastic growth model with a time scale that reverts to τ_{acc} (Fig. 2). Although such a model is satisfactory for the terrestrial planets where orbit periods are shorter and the presence of the nebula is not required (e.g., Wetherill, 1990), stochastic time scales from eqn (5) are too long for the outer solar system. If the final assembly of runaway embryos proceeds via the stochastic accretion process, the overall time scale for the formation of the giant planets will still be determined by this slow terminal step. A number of suggestions of how to avoid this late-stage time problem have been made in the literature, some of which are listed below.

i. Increased surface density. The easiest "fix" is to simply postulate a larger surface density than can be accounted for from the observed planetary masses (Lissauer, 1987). Because of the $\sigma^{3/2}$ dependence of eqn (9), a five-fold increase in σ is sufficient to raise the runaway limit, M_R, by an order of magnitude. This would permit suitable giant planet cores to form directly from accretion runaway, obviating the need for a "late-stage" at all. However, this suggestion may introduce other problems as knotty as the one it solves. In particular, one must explain why the excess mass does not accrete into more numerous and/or larger cores than desired. It may be possible that Jupiter and Saturn ejected all the excess material from the solar system after they had completed their gas acquisition phase, but a convincing model of this has yet to be presented. If a more massive disk extended into the inner solar system as well, it would be more difficult ~~to~~ remove excess material so deep in the solar gravity well. On the other hand, excess material does seem necessary in the outer solar system to explain the accretion of Uranus and Neptune within the age of the solar system (Fernandez and Ip, 1984). Material ejection also provides a plausible origin for the Oort cloud (Duncun et al., 1987). Although this proposition has obvious merit, it is, perhaps, premature to claim, as do Lissauer and Stewart (1993), that "minimum-mass models of the solar nebula are headed towards the dustbin of history".

ii. Diffusive redistribution of water vapor. A novel idea was proposed by Stevenson and Lunine (1987) that capitalized on the advantage of a larger surface density, but avoided the overall burden of excess system mass. This scheme exploits the proximity of Jupiter to the supposed location of the water condensation boundary in the primordial nebula. Mild turbulence in the gas disk can cause diffusive mixing of the inner portion of the nebula across the condensation boundary. Water vapor is trapped as condensate, with the boundary acting as a "cold finger". The local build-up of ice will raise the surface density of solid material, permitting larger runaway objects to develop in the region. Although clever, there is an obvious shortcoming of this scheme; it leaves the existence of Saturn as a separate unsolved problem.

iii. Decreased critical core size. Instead of increasing the runaway limit, another approach is to lower the critical core size. Most models of giant planet formation indicate that a critical core size of order 10 or more earth masses is required before gas accretion begins to contribute significantly to the growth rate of the planet (Podolak et al., 1993 and references therein). However, in a short communication, Stevenson (1984) pointed out that this critical size might be lowered if (*i.*) the extended gas atmosphere developing about the protoplanet has a low grain opacity, allowing for a more efficient heat radiation, and (*ii.*) the mean molecular weight of the atmosphere is raised by a high water vapor content, presumably derived from the icy core and mixed through the atmosphere by convection. Stevenson concludes that a critical core size of the order of an earth mass or less is possible, bringing this within reach of the runaway process without a need to augment the surface density. Of course, there may be many such objects that form, but their further combination via impacts could proceed faster than the standard accretion model because the large gas component will increase their masses and therein increase the effective surface density appearing in eqn (4). In addition, an extended atmosphere may also contribute to a larger cross section for such objects. A possible draw back of this idea is that the onset of gas accretion may prove a self-limiting event through its lowering of the mean molecular weight of the atmosphere. Although intriguing, further modeling efforts along this idea have not been forthcoming. (Serious interest in this idea was probably not helped along by Stevenson's labeling of these objects as *"superganymedian puffballs"*.)

iv. Disk tidal torques. Rather than trying to eliminate the late-stage, it may be that important physics is missing from the model. A potentially influential mechanism is the tidal interaction of embryos with the remnant nebula through density waves (e.g, Goldreich and Tremaine, 1980; Hourigan and Ward, 1984; Ward, 1986, Korycansky and Pollack, 1993; Artymowicz, 1993a). Density wave torques are proportional to the square of the perturber's mass and become more important as embryos grow. Gradients in the gas disk result in a net disk torque that can cause orbital drift with a time scale , $\tau_{dw} = r/\dot{r}$, given by

$$\tau_{dw} \sim \frac{\Omega^{-1}}{C}(\frac{M_\odot}{M})(\frac{M_\odot}{\sigma_g r^2})(\frac{c}{r\Omega})^2 \tag{13}$$

where σ_g is the gas surface density, c is the sound speed, and C is a constant of order 1–10 that depends on the structural properties of the disk. For the values in table II, eqn (13) reads $\tau_{dw} \sim 2 \times 10^6 C^{-1}(M_\oplus/M)$ years. Thus, runaway objects may have considerable mobility over the $\sim 10^7$ year lifetime of the nebula. Density wave torques damp eccentricities on an even shorter time scale, i.e., $\tau^e_{dw} \sim \tau_{dw}(c/r\Omega)^2 \simeq 10^4(M_\oplus/M)$ years (Ward, 1988, 1989; Artymowicz, 1993b). Depending on the relative timing of the growth of runaway objects, at least two scenarios can be envisioned:

(1.) If the planetesimal disk converts into one with most of its mass contained in runaway objects, further growth again must occur from their mutual collisions. Since $\tau_{dw} \propto M^{-1}$, stochastic mass differences among the embryos would result in differential decay. This could generate further encounters *without* requiring the large eccentricities and inclinations of the standard stochastic model. Growth has a feedback effect in that the largest object migrates fastest and increases its competitive edge over the other embryos (Hourigan and Ward, 1984). If the orbital inclinations remain low compared to the Safronov equilibrium value, $I_S \sim v/r\Omega \sim 0.7(M/M_\oplus)^{1/3}\rho_p^{1/6}/\theta^{1/2}$, the growth time can be significantly shorter than τ_{acc}, i.e., $\tau \simeq \tau_{acc}(I/I_S)$, with a lower bound of $\tau_{swp} \sim (C\Omega)^{-1}(\mu_d\mu_g)^{-1}(c/r\Omega)^2 \simeq 10^5$ years set by the supply rate of accretable material (Hourigan and Ward, 1984; Ward, 1989).

(2.) Alternatively, if one runaway object develops ahead of the others in a local region, disk tidal torques may push the embryo into adjacent, unaccreted regions of the disk and breach the runaway limit (Ward and Hahn, 1995). In this case, growth may continue on a time scale closer to $\tau_{R'}$. To successfully push the embryo out of the gap it has cleared, the density wave torque from the nebula must be strong enough to override the confining torques from the planetesimal disk (e.g., Goldreich and Tremaine, 1982). If the nebula torque is too small, the runaway object is merely displaced from the center of the gap and is only slightly larger. However, if the nebula torque exceeds a critical value, the runaway object cannot be confined to a gap and continues to cannibalize the planetesimal disk. To date, estimates of the nebula tidal torque due to density wave interactions generally exceed this critical strength (Ward, 1986; Korycansky and Pollack, 1993; Artymowicz, 1993a). The eventual onset of gas accretion when the embryo reaches core size will create local gradients in the nebula that will effectively abort the nebula torque and stabilize the protoplanet's orbit.

5. Summary

The overall sequence of events believed to lead to the formation of a planetary object can be split into three stages each characterized by different mechanisms of accumulation. The best understood of these is the mid-stage which describes the growth of planetary embryos of radii $\mathcal{O}(10^3)$ km from kilometer sized planetesimals. The primary growth mechanism is binary accretion where the inelastic nature of a collision between projectile and target dissipates enough energy that (most of) the collision products are gravitationally bound. Numerical models of the velocity and size evolution of a planetesimal swarm indicate that runaway growth of a few, stochastically larger objects is likely. Gravitational focussing causes a strong feedback in the enhancement factor (normalized cross section) so that runaway growth accelerates until limited by the stirring effects of the embryo. In the jovian zone, the maximum value of the enhancement factor is $F_g \sim \mathcal{O}(10^3)$ and the growth time is $\tau_{R'} \sim 4 \times 10^5 (R'/10^3 \text{ km})$ years. The mid-stage may terminate when local mass exhaustion limits embryo growth to $M_R \sim 2M_\oplus$.

Our knowledge is less complete for both the early and late stages of planetary accretion. Growth from μm$\rightarrow$cm sized planetesimals can be accomplished by a variety of non-gravitational mechanisms such as van der Waals bonding, electrostatic and magnetic forces, but accounting for growth to kilometer size planetesimals is still a theoretical challenge. Doubt has been cast on the gravitational instability mechanism by new numerical simulations of gas-particle dynamics in the solar nebula. These results indicate that turbulence may keep the planetesimal disk too thick for gravitational instability to develop. However, a suitable alternative mechanism to account for the coagulation of cm sized particles up to kilometer size is still lacking.

Late stage accretion has another set of problems. If accretion runaway stalls from local mass exhaustion, the disk becomes populated with $\sim \mathcal{O}(M_\oplus)$ sized embryos. For crossing orbits generated by gravitational relaxation of the disk, the large eccentricities and inclinations result in low collision probabilities. These imply unacceptably long growth times for the $\sim$ 15–30$M_\oplus$ cores of the giant planets which must form within the $\mathcal{O}(10^7)$ year lifetime of the gas disk. This late stage could be avoided if the surface density of solids was about five times larger than the nominal ~ 4 g/cm^2 usually assumed. If this case, runaway growth could produce cores capable of gas accretion directly. However, roughly 80% of the solid material would have to be ejected from the system by the newly formed giant planets before this material can follow a similar evolution into other large planetary objects. Other suggestions for avoiding the late stage involve lowering the critical core size for gas accretion and concentrating water ice in the jovian zone by diffusive redistribution of water vapor across the ice condensation boundary in the nebula.

Alternatively, density wave interaction with the remnant nebula may furnish an additional source of mobility for solid material that could shorten the late-stage. Disk torques damp embryo eccentricities as well as decay semi-major axes. The rates are proportional to the embryo's mass so that differential drift may force encounters even if orbits are nearly circular. This may lead to either continued runaway, if an embryo drifts into unaccreted region of the planetesimal disk; or to collisions between embryos themselves over a time scale shorter than the "standard" stochastic model. These are just a few ideas deserving of closer scrutiny.

Acknowledgments. This research was supported by NASA under Contract NBAS7-100 with the Jet Propulsion Laboratory, California Institute of Technology.

6. Appendix

The generalization of the growth time $\tau \equiv R_i/\dot{R}_i$, taking into account the finite sizes of both bodies, is

$$\tau_i^{-1} = \frac{1}{4}\frac{\rho}{\rho_p}\frac{v_{rel,i}}{R_i}(1+\frac{R}{R_i})^2\left[1+(\frac{v_{e,i}}{v_{rel,i}})^2\right] \tag{14}$$

where $R_i = (R, R')$, $v_{e,i}^2 = 2G(M+M_i)/(R+R_i)$ and $v_{rel,i}^2 = v^2 + v_i^2$. The dispersion velocity for the small field particles is given by $v^2 = GM/\theta R$, while the dispersion velocity for the large particles, v'^2, depends on whether or not there is equipartition of energy. We consider two extreme cases: equal velocity ($v'^2 = v^2$) and equal energy ($M'v'^2/2 = Mv^2/2$).

The ratio of growth times τ/τ' is given by

$$\frac{\tau}{\tau'} = \frac{1}{\lambda}(\frac{1+\lambda}{2\lambda})^2\sqrt{\frac{1+\chi}{2}}\left[\frac{1+2\theta(1+\lambda^3)/(1+\chi)(1+\lambda)}{1+\theta}\right] \tag{15}$$

where $\lambda \equiv R'/R$ and $\chi \equiv (1, \lambda^{-3})$ for the cases of equal velocities and equal energies, respectively. Runaway growth occurs when $d\lambda/dt > 1$. Since

$$\frac{d\lambda}{dt} = \frac{\dot{R}'}{R} - \frac{R'\dot{R}}{R^2} = \frac{\lambda}{3\tau}(\frac{\tau}{\tau'} - 1) \tag{16}$$

the derivative will be positive when $\tau/\tau' > 1$. Note that this ratio is identically one for $\lambda = 1$. For equal velocities, eqn (14) simplifies to

$$\frac{\tau}{\tau'} = \frac{1}{\lambda}(\frac{1+\lambda}{\lambda})^2\left[\frac{1+\theta(1+\lambda^3)/(1+\lambda)}{1+\theta}\right] \tag{17}$$

This exceeds unity for $\lambda > \lambda_{crit}^v$ where λ_{crit}^v satisfies

$$\theta = \frac{4\lambda^3 - (\lambda+1)^2}{(\lambda^3+1)(\lambda+1) - 4\lambda^3}. \tag{18}$$

Figure (6) displays $\lambda_{crit}^v(\theta)$. For the equal energy case

$$\frac{\tau}{\tau'} = \frac{1}{\lambda}(\frac{1+\lambda}{2\lambda})^2\sqrt{\frac{\lambda^3+1}{2\lambda^3}}\left[\frac{1+2\theta\lambda^3/(1+\lambda)}{1+\theta}\right] \tag{19}$$

which is greater than one for $\lambda > \lambda_{crit}^E$, where λ_{crit}^E satisfies

$$\theta = \frac{4\lambda^3 - (\lambda+1)^2\sqrt{(1+\lambda^{-3})/2}}{2\lambda^3(\lambda+1)\sqrt{(1+\lambda^{-3})/2} - 4\lambda^3}. \tag{20}$$

This relationship is also shown in figure (6).

References

Artymowicz, P. 1987. Self-regulating planetary growth. *Icarus* **70** 303–318.

Artymowicz, P. 1993a. On the wave excitation and a generalized torque formula for Lindblad resonances excited by external potential. *Astrophys. J.* **419** 155–165.

Artymowicz, P. 1993b. Disk–satellite interaction via density waves and the eccentricity evolution of bodies embedded in disks. *Astrophys. J.* **419** 166–180.

Aarseth, S. J., D. N. C. Lin, and P. L. Palmer 1993. Evolution of planetesimals. II. Numerical simulation. *Astrophys. J.* **403** 351–376.

Barge, P., and R. Pellat 1991. Mass spectrum and velocity dispersion during planetesimal accumulation: I. Accretion. *Icarus* **93** 270–287.

Blum, J. and M. Munch 1993. Experimental investigations on aggregate–aggregate collisions in the early solar nebula. *Icarus* **106** 151–167.

Burns, J. A., R. A. Kolvoord, and D. P. Hamilton 1989. An assessment of potential hazards to the Cassini spacecraft from debris along satellite orbits. In *Cassini Mission Announcement of Opportunity*, OSSA–1–89. JPL PD 699–11, Vol. 13, pp. 6.1–6.20.

Cuzzi, J. N., A. R. Dobrovolskis, and J. M. Champney 1993. Particle–gas dynamics in the midplane of a protoplanetary nebula. *Icarus* **106** 102–134.

Donn, B. 1990. The formation and structure of fluffy cometary nuclei from random accumulation of grains. *Astron. Astrophys.* **235** 41–446.

Duncan, M., T. Quinn, and S. Tremaine 1987. The formation and extent of the solar system comet cloud. *Astron. J.* **94** 1330–1338.

Fernandez, J. A. and W.–H. Ip 1984. Some dynamical aspects of the accretion of Uranus and Neptune: The exchange of orbital angular momentum with planetesimals. *Icarus* **58** 109–120.

Greenberg, R. J. 1989. Planetary accretion. In *Origin and Evolution of Planetary Atmospheres* (Eds., S. K. Atrya, J. B. Pollack, and M. S. Matthews) Univ. of Arizona Press, pp. 137–164.

Greenberg, R. J. , W. F. Bottke, A. Carusi, and G. B. Valsecchi 1991. Planetary accretion rates: Analytical derivation. *Icarus* **94** 98–111.

Greenberg, R., J. Wacker, W. K. Hartmann, and C. R. Chapman 1978. Planetesimal to planets: Numerical simulation of collisional evolution. *Icarus* **35** 1–26.

Greenberg, R., S. J. Weidenschilling, C. R. Chapman, and D. R. Davis 1984. From icy planetesimal to outer planets and comets. *Icarus* **59** 87–113.

Greenberg, R. S., A. Carusi, and G. B. Valsecchi 1988. Outcomes of planetary close encounters: A systematic comparison of methodologies. *Icarus* **75** 1–29.

Greenzweig, Y. and J. J. Lissauer 1993. Accretion rates of protoplanets. *Icarus* **87** 40–77.

Goldreich, P. and S. Tremaine 1980. Disk–satellite interactions. *Astrophys. J.* **241** 425–441.

Goldreich, P. and S. Tremaine 1982. The dynamics of planetary rings. *Annu. Rev. Astron. Astrophys.* **20** 249–283.

Goldreich P. and W. R. Ward 1973. The formation of planetesimals. *Astrophys. J.* **183** 1051–1061.

Hayashi, C., K. Nakazawa, and I. Adachi 1977. Long–term behavior of planetesimal and the formation of the planets. *Pub. Astron. Soc. Jpn.* **29** 163–196.

Henon, M. and J.–M. Petit 1986. Series expansions for encounter–type solutions of Hill's problem. *Celest. Mech.* **38** 67–100.

Horedt, G. P. 1985. Late stages of planetary accretion. *Icarus* **64** 295–307.

Hornung, P., R. Pellat, and P. Barge 1985. Thermal velocity equilibrium in the protoplanetary cloud. *Icarus* **64** 295–307.

Hourigan, K. and W. R. Ward 1984. Radial migration of preplanetary material: Implications for the accretion time scale problem. *Icarus* **60** 29–39.

Ida, S. 1990. Stirring and dynamical friction rates of planetesimals in the solar gravitational field. *Icarus* **88** 129–145.

Ida, S. and J. Makino 1993. Scattering of planetesimal by a protoplanet: slowing down of runaway growth. *Icarus* **106** 210–227.

Kaula, W. M. 1979. Equilibrium velocities of a planetesimal population. *Icarus* **40** 262–275.

Kolvoord, R. A. and R. Greenberg 1993. A critical reanalysis of planetary accretion models. *Icarus* **98** 2–19.

Korycansky,D. G. and J. B. Pollack 1993. Numerical calculations of the linear response of a gas disk to a protoplanet. *Icarus* **102** 105–165.

Levin, B. J. 1978. Relative velocities of planetesimal and the early accumulation of planets. *The Moon and the Planets* **19** 289–296.

Lissauer, J. J. and G. R. Stewart 1992. Growth of planets from planetesimal. In *Protostars and Planets III*, Eds. E. H. Levi and J. I. Lunine (Univ. of Arizona Press, Tucson).

Mizuno, H. 1989. Grain growth in the turbulent accretion disk nebula. *Icarus* **80** 189–201.

Nakagawa, Y., C. Hayashi, and K. Nakazawa 1983. Accumulation of planetesimal in the solar nebula. *Icarus* **54** 361–376.

Nishida, S. 1983. Collisional processes of planetesimal with a protoplanet under the gravity of the proto–sun. *Prog. Theor. Phys.* **70** 93–105.

Ohtsuki, K., and S. Ida 1990. Runaway planetary growth with collision rate in the solar gravitational field. *Icarus* **85** 499–511.

Ohtsuki, K., Y. Nakagawa, and K. Nakazawa 1990. Artificial acceleration in accumulation due to coarse mass–coordinate divisions in numerical simulation. *Icarus* **83** 205–215.

Ohtsuki, K. , Y. Nakagawa, and K. Nakazawa 1988. Growth of the earth in nebular gas. *Icarus* **75** 552–565.

Safronov, V. S. 1972. *Evolution of the protoplanetary cloud and the formation of the Earth and planets.* (Transl. Isreal Program for Scientific Translation, NASA TTF–677). Nauka, Moscow.

Sekiya, M. 1983. Gravitational instabilities in a dust–gas layer and formation of planetesimal in the solar nebula. *Prog. Theor. Phys. Suppl.* **69** 1116–1130.

Spaute, D., S. J. Weidenschilling, D. R. Davis, and F. Marzari 1991. Accretional evolution of a planetesimal swarm: 1. A new simulation. *Icarus* **92** 147–164.

Stevenson, D. 1984. On forming the giant planets quickly (superganymedian puff balls). 1984. *Lunar Planet. Sci. XV* 822–823.

Stevenson, D. and J. I. Lunine 1988. Rapid formation of Jupiter by diffusive redistribution of water vapor in the solar nebula. *Icarus* **75** 146–155.

Stewart, G. R. and G. W. Wetherill 1988. Evolution of planetesimal velocities. *Icarus* **74** 542–553.

Ward, W. R. 1986. Density waves in the solar nebula: Differential Lindblad torque. *Icarus* **67** 164–180.

Ward, W. R. 1988. On disk–planet interactions and orbital eccentricities. *Icarus* **73** 330–348.

Ward, W. R. 1989. On the rapid formation of giant planet cores. *Astrophys. J. Lett.* **345** 99–102.

Ward, W. R. 1993. Density waves in the solar nebula: Planetesimal velocities. *Icarus* **106** 274– 287.

Ward, W. R. and J. M. Hahn 1995. Disk tides and accretion runaway. *Astrophys. J. Lett.*, **440**, L25–28.

Weidenschilling, S. J. 1974. A model for accretion of the terrestrial planets. *Icarus* **22** 426–435.

Weidenschilling, S. J. 1977. Aerodynamics of solid bodies in the solar nebula. *Mon. Not. R. Astron. Soc.* **180** 179–188.

Weidenschilling, S. J. 1980. Dust to planetesimal: Settling and coagulation in the solar nebula. *Icarus* **44** 172–189.

Weidenschilling, S. J. 1984. Evolution of grains in a turbulent solar nebula. *Icarus* **60** 555–567.

Weidenschilling, S. J. 1988. Formation processes and timescales for meteorite parent bodies. In *Meteorites and the Early Solar System* (Eds. J. F. Kerridge and M. S. Matthews) Univ. Arizona Press, Tucson.

Weidenschilling, S. J. and J. N. Cuzzi 1993. Formation of planetesimals in the solar nebula. In *Protostars and Planets III*, Eds. E. H. Levi and J. I. Lunine (Univ. of Arizona Press, Tucson).

Wetherill, G. W. 1980. Formation of the terrestrial planets. *Annu. Rev. Astron. Astrophys.* **18** 77–113.

Wetherill, G. W. 1990. *Formation of the Earth. Annu. Rev. Earth Planet Sc.* **18** 77–113.

Wetherill, G. W. and G. R. Stewart 1989. Accumulation of a swarm of small planetesimal. *Icarus* **77** 330–357.

Wetherill, G. W. and G. R. Stewart 1993. Formation of planetary embryos: Effects of fragmentation, low relative velocities, and independent variation of eccentricity and inclination. *Icarus* **106** 190–209.